Naval Research Laboratory
Stennis Space Center, MS 39529-5004

NRL/FR/7180--00-9697

A Phenomenological Model to Predict the Density and Distribution of Pacific Hake by Season and Geography

REDWOOD W. NERO

Acoustic Simulation, Measurements, and Tactics Branch
Acoustics Division

March 20, 2000

REPORT DOCUMENTATION PAGE

Form Approved
OMB No. 0704-0188

1. AGENCY USE ONLY (*Leave Blank*)	2. REPORT DATE	3. REPORT TYPE AND DATES COVERED
	March 20, 2000	Final February 1992 to January 1999

4. TITLE AND SUBTITLE

A Phenomenological Model to Predict the Density and Distribution of Pacific Hake by Season and Geography

5. FUNDING NUMBERS

PE -0602435N
UW-35-2-09
Work Unit Number 6835

6. AUTHOR(S)

Redwood W. Nero

7. PERFORMING ORGANIZATION NAME(S) AND ADDRESS(ES)

Naval Research Laboratory
Stennis Space Center, MS 39529-5004

8. PERFORMING ORGANIZATION REPORT NUMBER

NRL/FR/7180--00-9697

9. SPONSORING/MONITORING AGENCY NAME(S) AND ADDRESS(ES)

Office of Naval Research
800 North Quincy Street
Arlington, VA 22217-5660

10. SPONSORING/MONITORING AGENCY REPORT NUMBER

11. SUPPLEMENTARY NOTES

12a. DISTRIBUTION/AVAILABILITY STATEMENT

Approved for public release; distribution unlimited.

12b. DISTRIBUTION CODE

13. ABSTRACT (*Maximum 200 words*)

A model has been developed to describe the migration and spatial distribution of hake at a time resolution of a month and at a spatial resolution of 10 km. The migration is empirical, with scaling parameters based on known endpoints and anecdotal observations from the fishery. Oceanographic and bathymetric data at a spatial resolution of 10 km are used as a geographic framework in which the migration is placed, allowing the formation of raster images of fish density. A swimbladder scattering model is used to convert fish density images to low-frequency volume scatter images. Model predictions match data with a ± 3 dB accuracy for most locations but with some sites still poorly predicted. Complex features of fish behavior and migration and interaction with oceanography are suggested as the cause of the disparity. The model is suggested as useful for generalized volume scattering predictions over shelf-wide geographic areas in seasons or locations where volume scattering data are sparse.

14. SUBJECT TERMS

Volume scattering Antisubmarine warfare
Fish migration
Fish distribution

15. NUMBER OF PAGES

22

16. PRICE CODE

17. SECURITY CLASSIFICATION OF REPORT	18. SECURITY CLASSIFICATION OF THIS PAGE	19. SECURITY CLASSIFICATION OF ABSTRACT	20. LIMITATION OF ABSTRACT
UNCLASSIFIED	UNCLASSIFIED	UNCLASSIFIED	UL

NSN 7540-01-280-5500

Standard Form 298 (Rev. 2-89)
Prescribed by ANSI Std 239-18
298-102

CONTENTS

A PHENOMENOLOGICAL MODEL TO PREDICT THE DENSITY AND DISTRIBUTION OF PACIFIC HAKE BY SEASON AND GEOGRAPHY

INTRODUCTION

Fish cause volume reverberation, clutter, and false targets and can interfere with the performance of Naval active sonar systems. This interference is especially strong in continental shelf and slope waters where the abundance of fish is far greater than in the open ocean. An ability to predict the occurrence of fish and the potential for biological causes of reverberation, clutter, and false targets would provide environmental knowledge useful for Navy planning.

Pacific hake, *Merluccius productus*, are the single largest stock of fish on the U.S. west coast. They occur in midwater on the continental shelf and slope from Baja California to Queen Charlotte Sound. Pacific hake provide a unique opportunity to test a simple model for predicting the abundance and distribution of a single fish stock and ultimately for predicting volume reverberation and false targets. If predictions from a single species model work reasonably well, then additional species models may be developed for shelfwide regions. Any model of fish prediction to be used by Naval antisubmarine warfare (ASW) and mine countermeasure (MCM) systems must be generally applicable in many parts of the world. For this reason, the models must be based on general observations that are obtainable for other stocks of fish where some of the basic biological parameters are poorly known.

To meet this criterion of wide applicability, a migration model was derived from a set of general observations about the west coast hake population. It consists of a set of empirical formulas allowing the calculation of the expected number of hake at a particular latitude in a particular month. It was designed to fit the known observations of hake distribution and migration without any regard to the mechanisms of the migration. More detailed biological mechanism- oriented models may be found in Francis (1983) and Smith et al. (1992).

Calculations are made in a geographic framework to allow the derivation of maps of fish density and depth. These maps are coupled to a swimbladder resonance model (Love 1978) to provide maps of expected volume scattering. Finally, volume scattering values predicted by the model are compared to measurements obtained at sites visited by the Naval Research Laboratory (NRL) in August 1992 and July 1995.

MIGRATION AND DISTRIBUTION OF PACIFIC HAKE

The Seasonal Migration

Much of our knowledge of Pacific hake comes from a recent review of Pacific hake (Methot and Dorn 1995), surveys conducted by the National Marine Fisheries Service (NMFS), and observations made by fishing fleets (Stauffer 1985). Hake undergo a seasonal migration. Adult fish spend the winter on spawning grounds between Point Conception and Baja California. In the spring, after the fish have spawned, they begin migrating north to feed in the productive waters along the continental shelf from northern California to Vancouver Island. They remain on the feeding grounds through the summer. In the autumn, the adults migrate south back to Baja. Juvenile fish mimic the migratory pattern of the adults but exhibit a migration pattern of reduced amplitude, spending the winter in southern California and migrating only as far north as southern Oregon in summer.

Manuscript approved May 5, 1999.

Knowledge of this general pattern is augmented by numerous anecdotal observations. Observations from the Soviet fishing fleet during 1965-69 (Ermakov 1974) indicate that post-spawn hake begin to appear just north of San Francisco in mid March. Ermakov's report suggests hake migrate in large schools that show up off Oregon and Washington in mid April and off Vancouver Island by late May. The schools appear to migrate northward at 6 to 11 km/day, following the edge of the continental slope. In June, the schools expand shoreward, with some schools occurring as shallow as 90 m. Dense feeding aggregations of hake occur from April to November along the shelf break off Oregon and Washington (Methot and Dorn 1995). In the fall, the migration is reversed with hake moving offshore and then southwards along the slope (Stauffer 1985).

The timing of the migration can vary by a month or more, depending on local coastal currents and weather. Soviet catch statistics show that fish may be present off Vancouver Island and Washington as early as January in some years and, in other years, may stay as late as December. A substantial catch was taken during November in three of 10 years between 1967 and 1976 (Beamish and McFarlane 1985).

Hake aggregate isobathically on the summer feeding grounds, with the greatest aggregations over bottom depths of 50 to 100 m. However, hake continue to occur out to bottom depths of about 300 m. Based on bottom trawl catches and acoustic surveys, large aggregations can occur at bottom depths near 200 m (Nelson and Dark 1985; Methot and Dorn 1995). The summer aggregations are associated with the occurrence of euphausiids (Mackas et al. 1997) and occur at temperatures between 5 °C and 9 °C (Swartzman 1997; Mackas et al. 1997) with peak concentrations occurring at about 6 °C (NRL, unpublished data).

Vertical Distribution

When feeding, hake undergo diurnal migrations, apparently in response to the vertical migration of euphausiids, their primary food (Stauffer 1985; Simard and Mackas 1989; Mackas et al. 1997). They aggregate in dense schools at depths of 100 to 250 m during the day. At night some of the hake migrate upward and spread into a diffuse layer between 250 m and the surface (Stauffer 1985). NRL data corroborate these general depth ranges (Nero et al. 1998) but also suggest that their vertical distribution is centered near the 6 °C isotherm (NRL unpublished data). The vertical distribution of hake is not documented for the northward or southward migrations. During spawning in February hake do not feed and remain at depths of 150 to 400 m (Saunders and McFarlane 1997). Shortly after spawning hake have been caught with food in their stomachs (Saunders and McFarlane 1997), suggesting that feeding and vertical migrations resume after spawning.

Abundance

Extensive acoustic surveys have been carried out every three years since 1977 by the NMFS to assess Pacific hake abundance (Francis and Hollowed 1985). These surveys are carried out in conjunction with an extensive bottom trawl survey. In combination, the two techniques are used to provide an estimate of hake density and abundance. The hake population is dynamic, often several weak year classes are followed by a strong year class, so that a majority of the population at any time may be dominated by a few strong year classes. In 1992, the hake population was dominated by fish from strong year classes in 1984, 1987, and 1990 (Dorn et al. 1994). By 1995, the hake population gained fish from a strong year class in 1993 (Wilson and Guttormsen 1997).

Several theories in fisheries ecology suggest that an upper limit on fish density occurs because of space dependent ecological constraints and that fish populations maintain a high and constant local density near the center of their optimal habitat (MacCall 1990). The overall area distribution contracts as the population becomes smaller. Pitcher and Alheit (1995) suggest that because of a hake's unique feeding behavior, ambush predation, and high cannibalism, this may not be the case for hake. Hake may rather tend to occupy a large region, with local density dependent on overall population abundance. As the population becomes smaller, the hake occupy the same region but at a lower density. However, the most recent acoustic surveys of the US-west coast hake population suggest an upper limit on their

maximum density. Acoustic measurements at 5 kHz suggest that an average hake density is roughly 0.05 indiv./m^2 with dense concentrations near 0.15 indiv./m^2 (Nero et al. 1998).

MODEL

Primary Model

In this report, predictions are made of the proportion of the hake population by age, month, latitude, and distance inshore and offshore from a migration corridor. Raster based maps are used to build and represent the migration corridor. All maps are 512 × 512 pixel raster images of a 45° latitude by 45° longitude area with the NW corner point at 55.28° N 146.55° W, and the SE corner point at 10.28° N, and 101.55° W. From overall abundance data predicted proportions are translated into fish numbers and a model of swimbladder resonance is used to generate a raster image of volume reverberation. The corresponding image resolution is such that each pixel corresponds to an approximate 10 km × 10 km area. The calculation of the migration is split into two parts: the first determines the position of fish in the north-south along-shelf direction, and the second determines the inshore-offshore across-shelf distribution. Calculations use maps of bathymetry derived from the US. Navy Digital Bathymetric Database (DBDB) at a 5-km resolution. The bathymetry was used to define a migration corridor that is based on the position of the shelf-slope break. The vertical position of the population is based on thermal structure, where the mean vertical position is centered on the depth of the 6 °C isotherm as determined from the U.S. Navy Generalized Digital Environmental Model (GDEM), as applied to sea surface temperatures for August 1992.

The backscattering for a layer of fish for month t, at pixel location x (longitude), and y (latitude) is given by

$$SL_{txy} = 10\log_{10}\sum_{i=1}^{m}\sum_{z=1}^{n}\sigma_{iz}\cdot\delta_{iztxy}\ , \tag{1}$$

where there are m age classes and n depth layers, σ_{iz} is the backscattering from an individual fish (of age i, at depth z) calculated for frequencies of interest using formulas in Love (1978), and δ_{iztxy} is the areal density of fish in the nth layer. For Pacific hake, we have chosen m = 10 and n = 13. The 10th age class contains all fish from ages 10 through 15 because there are fewer older fish and they are similar in size. Calculation of σ_{iz} requires information on fish size and acoustic properties.

At each pixel, the range of depths that fish can occur varies depending on thermal structure and bottom depth. The allocation of fish to depth layers at pixel x, y, is proportional to layer thickness such that,

$$\delta_{iztxy} = \frac{\Delta Z_n \delta_{itxy}}{\Delta Z_T}\ , \tag{2}$$

where ΔZ_n is the thickness of layer n, and ΔZ_T is the total depth range of hake. The 13 standard depth layers were defined as: 0 to 10 m, 10 to 14 m, 14 to 20 m, 20 to 28 m, 28 to 40 m, 40 to 56 m, 56 to 80 m, 80 to 112 m, 112 to 160 m, 160 to 224 m, 224 to 320 m, 320 to 448 m, and 448 to 640 m. The current model is limited to 640 m. Fish were placed at equal concentrations into only those depth layers which overlap with the predicted depth range of the hake. The prediction of the depth range of the hake was based on a scheme where fish always occur near the 6 °C isotherm during the day but also includes vertical migration at night. The predicted depth range was based on a daytime preference for 50 m above and 50 m below the depth of the 6 °C isotherm and a nighttime preference for 150 m above and 50 m below the depth of the 6 °C isotherm. These depth preferences were restricted so that hake did not occur above the sea surface or below the seafloor. For lack of better information on vertical migration during their seasonal migration, the hake were modeled as migrating vertically during all months. Although not implemented here, vertical migration could be suppressed during February to better simulate the absence of a vertical migration at spawning.

In the model that follows, a number of empirical equations are presented which were derived based on "eye" fits to the known behavior of hake. Much of the information was anecdotal and the equations contain numerous parameters that are only mathematical functions used to describe a particular shape without regard to the actual underlying biological mechanisms. In particular, Eqs. (3) and (4), (9) through (12), and (15) through (17) contain such terms.

Migration Kernel

The kernel of the hake migration model is the term P_t, which describes the proportion of the distance traveled along the migration corridor at any time and is given by

$$P_t = \frac{1 - \cos\left(\frac{\left(t - t_{lag}\right)\pi}{6}\right)}{2}. \tag{3}$$

Equation (3) assumes the migration of hake along the corridor follows a simple cycle, analogous to the seasonal climactic cycle. This cycle is approximated by a simple sinusoid function where P_t is the proportion of the migration accomplished at calendar month t, with month values ranging from 1 through 12 for January through December, respectively, and t_{lag} is the time lag between the calendar month and the migration cycle. Since the Pacific hake migration starts in February, a value of $t_{\text{lag}} = 2$ is used for hake on the west coast. Equation (3) is plotted in Fig. 1, where values of P_t are 0 at the start of the migration in February, 0.5 midway through the migration in May and November, and 1 at the maximum extent in August. The sinusoid shape results in slow movement at the migration endpoints and maximum motion at its midpoint with the two sides of the cycle identical in shape. Hence, fish are in identical positions in the reciprocal months, for example June and October or April and December. Subsequent equations use P_t to scale the migration corridor, provide different migration rates for each age class, and to spread each cohort out along the length of the migration corridor. A simple index to measure the amount of migration completed at t, based on P_t is

$$\alpha_t = 0.25 - \left(P_t - 0.5\right)^2, \tag{4}$$

which is used in the calculation of several of these parameters. α_t has a value of 0 at the migration endpoints, February and August, and a value of 0.25 midway through the migration in May and November.

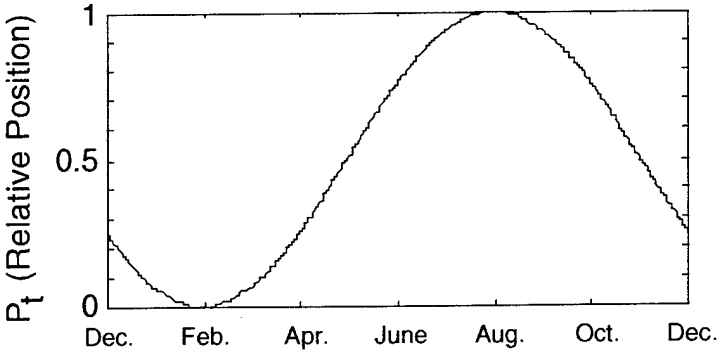

Fig. 1 — Curve depicting the basis of the yearly migration cycle

Migration Corridor

The migration corridor is a sinuous path of pixels running in a generally southeast to northwest direction roughly parallel to the shelf edge. It was created by applying several simple image processing steps to the map of west coast bathymetry. The bathymetric data were limited to a 22-m resolution because image representation of the data was restricted to integers between 1 and 512. The first step in defining the migration corridor was to obtain a slice of the bathymetric data between 3 and 9 units (66 to 198 m) to represent the outer continental shelf and shelf break. This region was then reduced to a corridor 1 pixel wide by applying an image processing "skelotonize" operation that eliminated all adjoining extraneous pixels. This gave a migration path which was an approximation of the middle of the outer shelf and shelf break. Determination of distance along the corridor was accomplished by assigning a single pixel at the southern tip of Baja California (23°N, 110°W) as a starting point. The range from this starting point to all other pixels on the map was calculated and assigned to a range map. This map had the appearance of a bullseye. Because the migration corridor was approximately linear in the SE to NW direction, the range map values corresponding to the pixels along the migration corridor gave the corresponding distance along the length of the corridor. Range steps c, cover 230 steps, from 1 at the southern starting point to 230 at the northern end (55°N, 135°W) with each step containing a segment of a torus encompassing approximately 2 pixels in the range direction and 50 to 100 pixels in the across-corridor direction. Range steps were used in subsequent along-corridor and across-corridor calculations.

Mean Position

A cohort's mean position at month t along the migration corridor is given by

$$m_{t,i} = s_i + P_t\left(f_i - s_i\right), \tag{5}$$

where f_i and s_i, are scaling parameters that are defined below. Although the shape of the migration is defined by Eq. (3), additional parameters in Eq. (5) are required to adjust the position and magnitude of the migration for each cohort and to scale the migration to the migration corridor.

Two parameters that define the mean position of an age group's most southern and northern position are $C_{spawn(i)}$ and $C_{feed(i)}$ (Table 1). Values of these parameters were derived from observations from the fishery based on Ermakov (1974), Smith et al. (1992), and Stauffer (1985). These values can be shifted northward or southward depending on whether the year being predicted is cooler or warmer than average and the hake's position of spawning or feeding is expected to occur more northwards or southwards than on average.

Scaling is accomplished by expressing all positions as relative to total path length of the migration corridor, where the overall southernmost position at which hake can occur is c_o (range step of 0) and the overall northernmost position is c_{max} (range step of 230). c_o and c_{max} set the limits by which all other parameters are scaled. Subsequent conversion of $C_{spawn(i)}$ to a relative distance measure is by the scaling parameters s_i and f_i,

$$s_i = \frac{c_{spawn(i)}}{c_{max} - c_0}, \tag{6}$$

and conversion of $C_{feed(i)}$ to a relative distance measure is by

$$f_i = \frac{c_{feed(i)}}{c_{max} - c_0}, \tag{7}$$

and any range step c's relative position along the corridor is given as

$$d_c = \frac{c}{(c_{\max} - c_0)}. \tag{8}$$

Table 1 — Endpoints for the Hake Migration by Age Group in Units of Latitude and Corridor Position (230 Range Steps Between 23°N and 55°N)

Age Group (yr)	$C_{spawn(i)}$		$C_{feed(i)}$	
	(latitude)	(range step)	(latitude)	(range step)
1	36.77	100	37.00	109
2	35.10	88	42.00	139
3	34.13	81	44.20	148
4	33.30	75	45.20	152
5	32.60	70	45.90	156
6	32.04	66	46.40	159
7	31.63	63	46.80	161
8	31.21	60	47.10	163
9	30.93	58	47.30	164
10	30.65	56	47.50	165
11	30.37	54	47.65	166
12	30.10	52	47.76	167
13	29.96	51	47.87	168
14	29.82	50	47.95	169

Equation (5) and the above endpoints were used to determine the distribution of fish over latitude (or steps) by month (Fig. 2). For each age class, a simple sine-wave was used to represent latitudinal position. The overall result provides a reasonable representation of the migration of hake from their overwintering area in the south (steps 50 to 100) to their summer feeding range in the north (steps 109 to 169). At both the southern and northern limits of the migration, the hake are distributed by age, with younger fish migrating shorter distances than older fish. Age 1 hake remain almost stationary, while each subsequently older year class travels farther north and farther south. The model gives reasonable estimates of migration rate, the slope of the curves in May in Fig. 2 suggest that age 1 hake are traveling at about 1 km/day, while the oldest and fastest hake, age 14, are traveling at about 16 km/day. These rates are reasonably close to observed movements of schools of older hake at 6 to 11 km/day (Ermakov 1974).

One additional measure based on f_i and s_i, is an index giving a relative measure of an age groups total migration path length

$$\beta_i = 0.1 \cdot (f_i - s_i)^2, \tag{9}$$

which is used as a weighting factor in the calculations which follow.

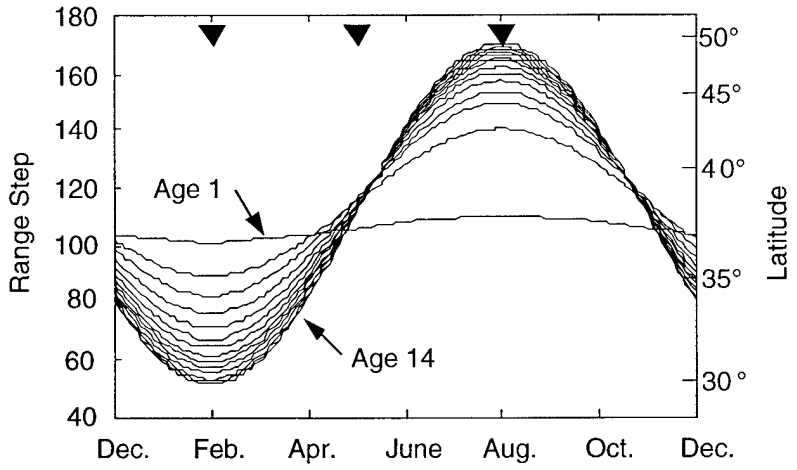

Fig. 2 — Mean position of each hake age group during their yearly migration cycle. Markers along top indicate months at which along-corridor spread is shown in Fig. 3.

Along Corridor Distribution

Equation (5) gives the mean position of an age group. However, natural variation in migration timing and fish swimming speed will smear the population along the migration path. The following equations provide for along corridor spreading about an age group's mean position. Thus, an index of hake occurrence at any relative position, d_C on the migration corridor is given by

$$P_{itc} = \frac{1}{e^{\gamma_{ti}(m_{ti}-d_c)^2}}, \tag{10}$$

where the term γ_{ti} is defined as

$$\gamma_{ti} = \frac{1}{\left(0.005+\left(\beta_i \cdot \alpha_t\right)\right)\cdot \omega_i}. \tag{11}$$

High values of β_i increase the spread throughout the migration cylce while high values of α_t increases the spread halfway through the migration cycle (May and November). The parameter

$$\omega_i = 2 - e^{-.6931\left(\frac{2B_i}{2700}\right)^{3.219}}, \tag{12}$$

increases the spread of an age group when its biomass (B_i) becomes excessively large. Values of ω_i range from 1 to 2 for corresponding biomass values of 0 to 2,700 mt.

Equation (10) results in the spread in an age group's distribution changing with the migration. In Fig. 2, time marks indicate where plots of the distribution of hake along the corridor in February, May, and August are shown in three panels in Fig. 3. Each panel gives the relative biomass of hake in age groups 1 to 14 by range step. The middle of each bell-shaped curve indicates an age group's mean position (m_{ti}). Spread in the curves indicates an age group's spread over range. Near the migration endpoints, February or August, the amount of spread in each age group is the smallest, and near the middle of the migration, May, the spread in each age group is the largest.

Biomass Along the Corridor

Equations (3) through (12) give the relative index of hake occurrence at a position on the migration corridor. Within range step c, a determination of the biomass for age i from the relative biomass, is determined as

$$B_{itc} = B_i \frac{P_{itc}}{\sum_{c=1}^{230} P_{itc}}, \tag{13}$$

with the total biomass of hake in that range step as

$$B_{tc} = \sum_{i=1}^{m} B_{itc}. \tag{14}$$

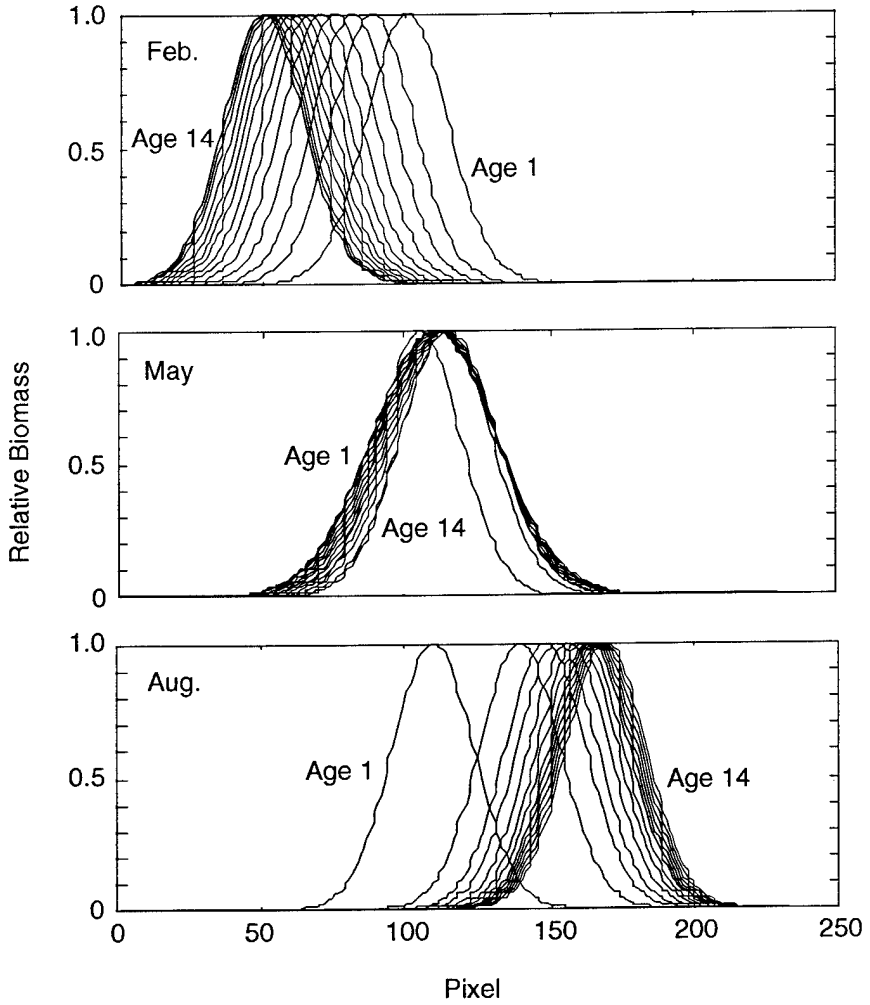

Fig. 3 — Relative biomass of hake along the migration corridor for age 1 to age 14

Across Corridor Distribution

Given the total biomass within a range step, the following equation is used to define the distribution of biomass of hake across the corridor

$$B_{tc} \approx \kappa_t \sum_{v=1}^{v_n} e^{-0.6931 \cdot \left(\frac{2v}{v_n}\right)^{3.219}}, \tag{15}$$

where the exponent describes a sigmoid-shaped curve with maximum density of hake near the corridor and minimum density away from the corridor. The density term κ_t is discussed below. To achieve the correct gradient in density, Eq. (15) is iteratively solved to determine v_n, the number of pixels in the range step c under the constraint that the sum of biomass from pixels within the range step equals the sum of biomass expected based on Eq. (14). The v_n pixels within a range step are ranked in order of distance away from the corridor, with inshore and offshore directions treated equally and pixels at depths less than 66 m ignored. Based on the shape described by Eq. (15), hake are assigned to each of the ranked pixels contained within that range step. Since each the elements of range step c are pixels with x and y coordinates, solving Eq. (15) gives the total biomass within each pixel such that $B_{tc} \Rightarrow B_{txy}$ (and $B_{itc} \Rightarrow B_{itxy}$). Figure 4 is an example for the shape in Eq. (15) for when v_n = 20 pixels.

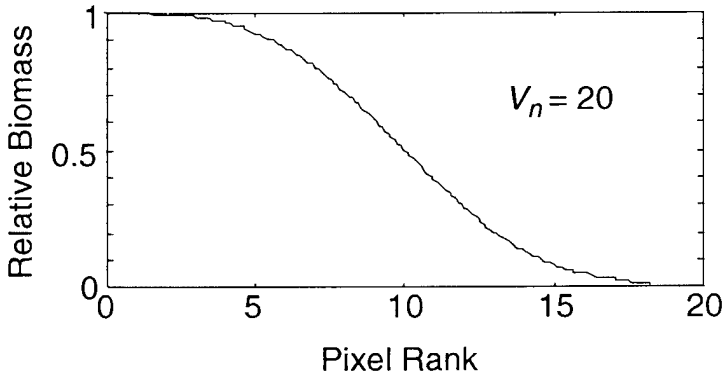

Fig. 4 — An example of the determination of the relative biomass to be assigned to each pixel within a range step c, on the migration corridor, when v_n = 20 pixels

The density term

$$\kappa_t = K + \xi_t^4 \cdot 10{,}000 \tag{16}$$

in Eq. (15) contains a constant K which is the optimal hake density, set at 5,000 tons/pixel (all cohorts included), and the term ξ_t gives the increase in density expected during the peak in migration,

$$\xi_t = \sin\left(\frac{(t - t_{lag})\pi}{6}\right), \tag{17}$$

where the term $\xi_t^4 \cdot 10,000$ ranges from 0 at the migration beginning or end (February or August) to 10,000 at its midpoints (May and November).

Density from Biomass

The density of hake at pixel x, y, is given by converting biomass to density

$$\delta_{itxy} = \frac{B_{itxy}}{W_i}, \tag{18}$$

where W_i is the average individual hake weight for cohort i, given by standard empirical relationships of hake weight (kg) to length, L_i, (cm)

$$W_i = 0.000015 L_i^{2.877}, \tag{19}$$

and hake length (cm) to age (years) (Dorn et al. 1994).

$$L_i = 60.85\left(1 - e^{-0.3(i-0.03)}\right). \tag{20}$$

Model Execution

During a model run, proportions at each pixel were translated to density estimates using Eq. (18) and stored as raster images of fish density. The numerical density of fish at each pixel was proportionally divided into depth strata (using Eq. (2)) and the resulting density of fish of age i, at depth z was used as input to the model of swimbladder resonance to generate estimates of volume scattter. Following Eq. (1), layer strengths were calculated for each pixel and maps of backscattering were generated for single layers. Layers were integrated to produce maps of total layer strength.

Raster image "skelotonizing," editing, and viewing were performed using public domain software "NIH Image" version 1.59 on a Macintosh. All other numeric computations and image manipulations were written in C and programs were controlled by executable shell scripts in Unix.

RESULTS

Comparison with Measurements

The hake model was run and compared for two surveys of volume scattering, the first in August 1992 and the second in July 1995 (Fig. 5). In August 1992, volume scattering was measured using the NRL USRD Model F55 line-hydrophone in conical reflector (described by Thompson and Love 1996), with survey results reported in Nero et al. (1998). The July 1995 measurements used a larger NRL USRD Model F78 line-hydrophone in reflector.

Comparative runs with the hake model were made using a total biomass of hake for 1992 and 1995 estimated from the results of a stock synthesis model (Table 16 in Dorn and Saunders (1997)). The stock synthesis model tracks age groups of fish through time, assuming average rates of fishing and natural mortality, and includes measurements of stock biomass when available. In Table 2, results of the stock synthesis model in numbers of fish were converted to biomass using the length-weight relationships (Eqs. (19) and (20)). Because the stock synthesis model does not provide estimates of the numbers of age 1 fish, their numbers were estimated from the numbers of age 2 fish in the subsequent years (1993 and 1996) by backcalculating to 1992 and 1995 assuming a 23% mortality rate (Dorn and Saunders 1997).

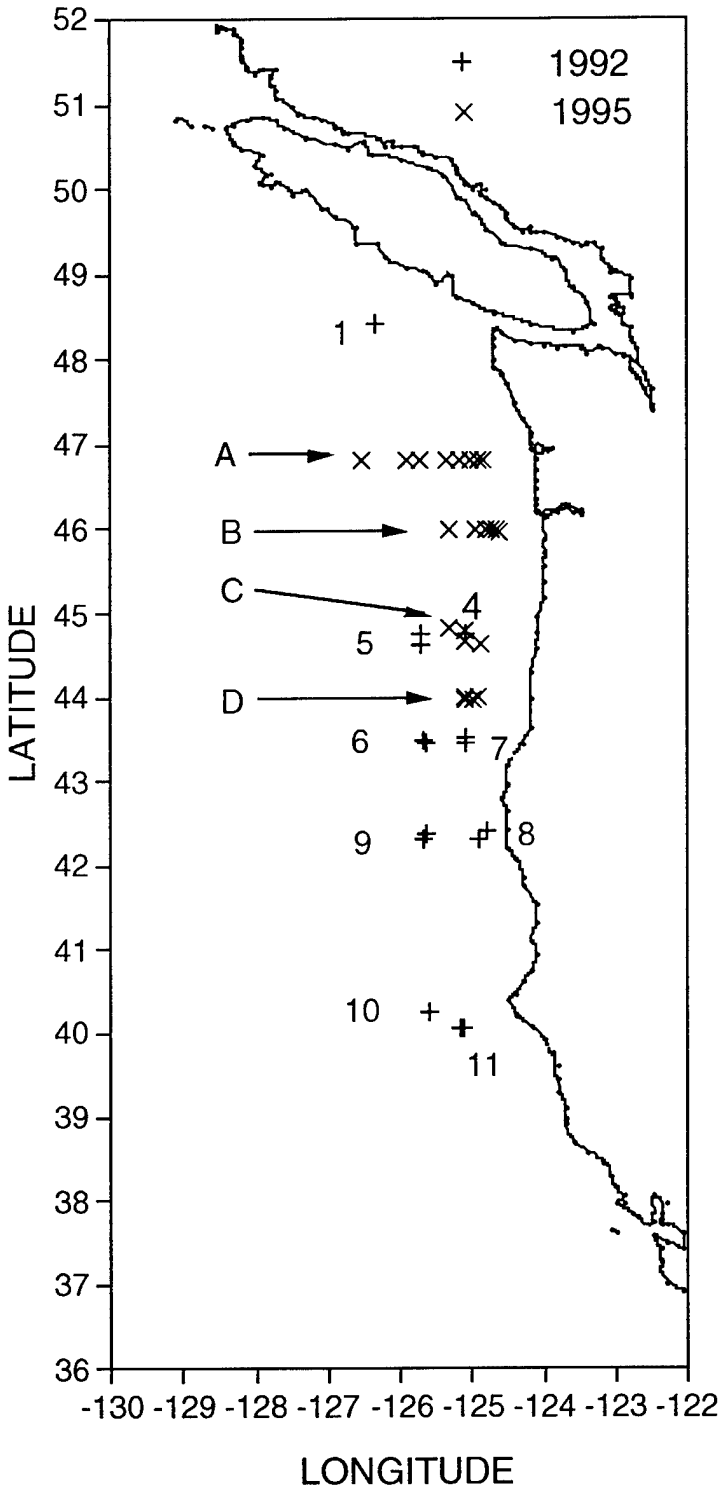

Fig. 5 — Volume scattering measurement stations in 1992 and 1995. Station order from shore seaward on the 1995 lines were A-5, 4, 3, 2, 1, 7, 6; B-3, 4, 5, 6, 7; C - 2, 3, 4, 5; and D-3, 2, and 1. Symbols on the map include locations for both night and day measurements.

Preliminary model runs were used to obtain a best fit to the volume scatter measurements. Because numerous adjustments were necessary for the model parameters, intermediate results are not shown, instead only the final adjustments and reasons for making them are given here. First, the total biomass of hake was increased by 80% to provide enough fish such that they would occur far enough offshore to match the volume scattering measurements. Nero et al. (1998) showed that the NMFS surveys were suspect of missing fish that occurred beyond the offshore limit of the surveys. Increasing the total hake biomass by 80% provided sufficient scattering at most offshore stations. Second, the mean positions of the summer feeding (Table 1), had to be adjusted 15 range steps southward (approximately 2° of latitude), to provide a better match of predicted volume scattering with measured volume scattering at the northernmost and southernmost NRL stations. The winter spawning positions (Table 1) were left unchanged.

Table 2 — Hake Numbers and Biomass Estimated from Results of a Stock Synthesis Model by Dorn and Saunders (1997) and Used as Input to the Hake Model

Age (yr)	Length (cm)	Weight (kg)	N (1992) (millions)	N (1995) (millions)	W (1992) (1000 mt)	W (1995) (1000 mt)
1	15.4	0.04	481	3147	19	122
2	27.2	0.20	1918	2169	384	434
3	35.9	0.45	168	133	75	59
4	42.4	0.72	732	217	526	156
5	47.1	0.98	1166	791	1141	774
6	50.7	1.21	136	61	164	73
7	53.3	1.40	31	234	43	326
8	55.3	1.55	1693	344	2618	532
9	56.7	1.67	30	39	50	65
10	57.8	1.76	10	9	18	15
11	58.6	1.83	25	483	46	884
12	59.2	1.88	613	9	1153	16
13	59.6	1.92	23	3	45	6
14	59.9	1.95	13	8	26	16
15	60.2	1.97	128	271	253	534

The coastwide distribution of hake biomass was modeled for February, May, and August 1992. The resulting curves shown in Fig. 6 include the change in each age group's latitudinal spread during the seasonal migration. The proportion of each age group at each latitude has been converted to actual biomass to demonstrate its effects on the spread of each cohort. The age 1 hake are more tightly grouped at either end of the migration in February or August, while during the peak in the migration in May, they are spread out. The biomass curves for the southward migration in November are not shown because they are the same as those for May.

Application of the hake model allowed the determination of volume scattering on a pixel by pixel basis, giving rise to maps of volume scattering. Figure 7 shows the predictions representing the change in the distribution of hake from spawning in February to feeding in August. This prediction was for the modified 1992 biomass of hake. Because the return migration southward is the reverse of the northward migration, it is not shown. The effect of allowing the maximum density of fish to rise from 5,000 tons/pixel to 15,000 tons/pixel during the peak of the migration in May is evident in this figure, where the hake are compressed into a narrow band along the shelf break in May. This presumably would occur if the hake migrate in large compact shoals as suggested by the observations of Ermakov (1974).

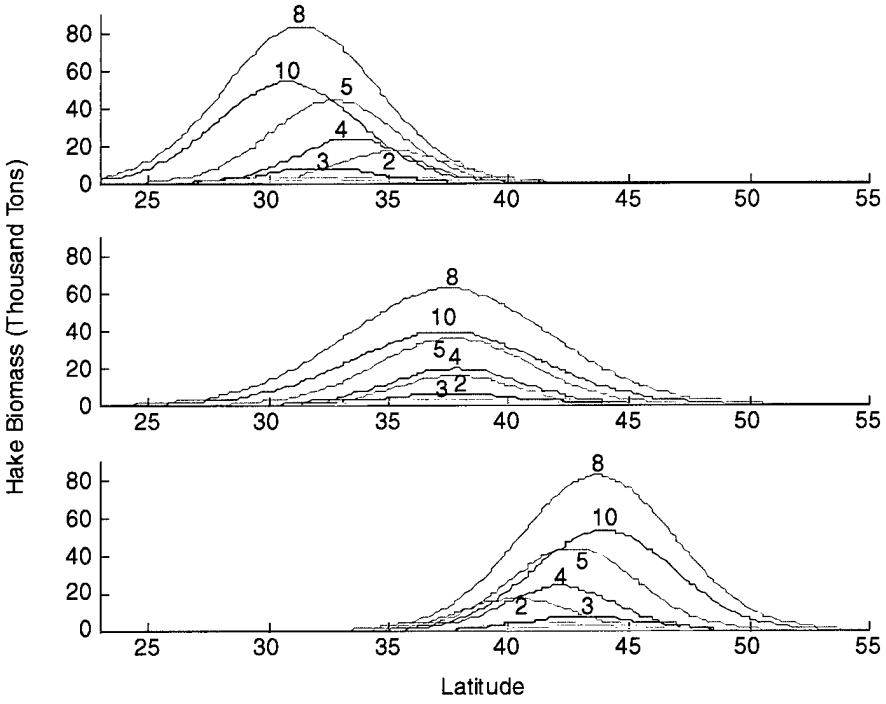

Fig. 6 — Predicted distribution of hake biomass over latitude. Numbers on curves indicate age groups. Biomass is for a latitude range corresponding to the width of one pixel (0.088°). Age groups 6, 9, 7, and 1, are hidden on the abscissa.

Figures 8 and 9 compare model predictions with August 1992 and July 1995 volume scatter measurements, respectively. In 1992 at all stations except 10, measurements compared reasonably well with the model. At station 10, the model appeared to provide a higher estimate by about 6 dB, or about four times as many fish as actually occurred. Station 10 was one of the farther offshore stations in the south of the study area, where the abundance of hake dropped off more rapidly than predicted by the model. This also occurred in 1995 at the offshore end of line A: the model predicted no hake at either A6 or A7, yet measurements showed low densities of hake at Station A7 (note, station A6 was seaward of A7). This suggests there still is an uncertainty in modeling the offshore limit of the hake in both 1992 and 1995. In addition to the problem of the offshore limit, a number of the 1995 stations showed other mismatches between the model and the data. Major model-data differences in overall level were evident at stations A1 and D3, with A1 showing the model too high and D3 showing the model too low. Discrepancies in resonance frequency also suggest that either the size of hake or their depth range appears to have been modeled incorrectly at stations A1, A5, and B3. At night in both 1992 and 1995, smaller scatterers, presumably mesopelagic fish, are responsible for a rise in scattering levels at frequencies above 2.5 kHz (especially evident at 1992 stations 5, 7, 9, and 11, and at 1995 stations A2, A3, B6, and B7). These fish were not included in the present modeling effort.

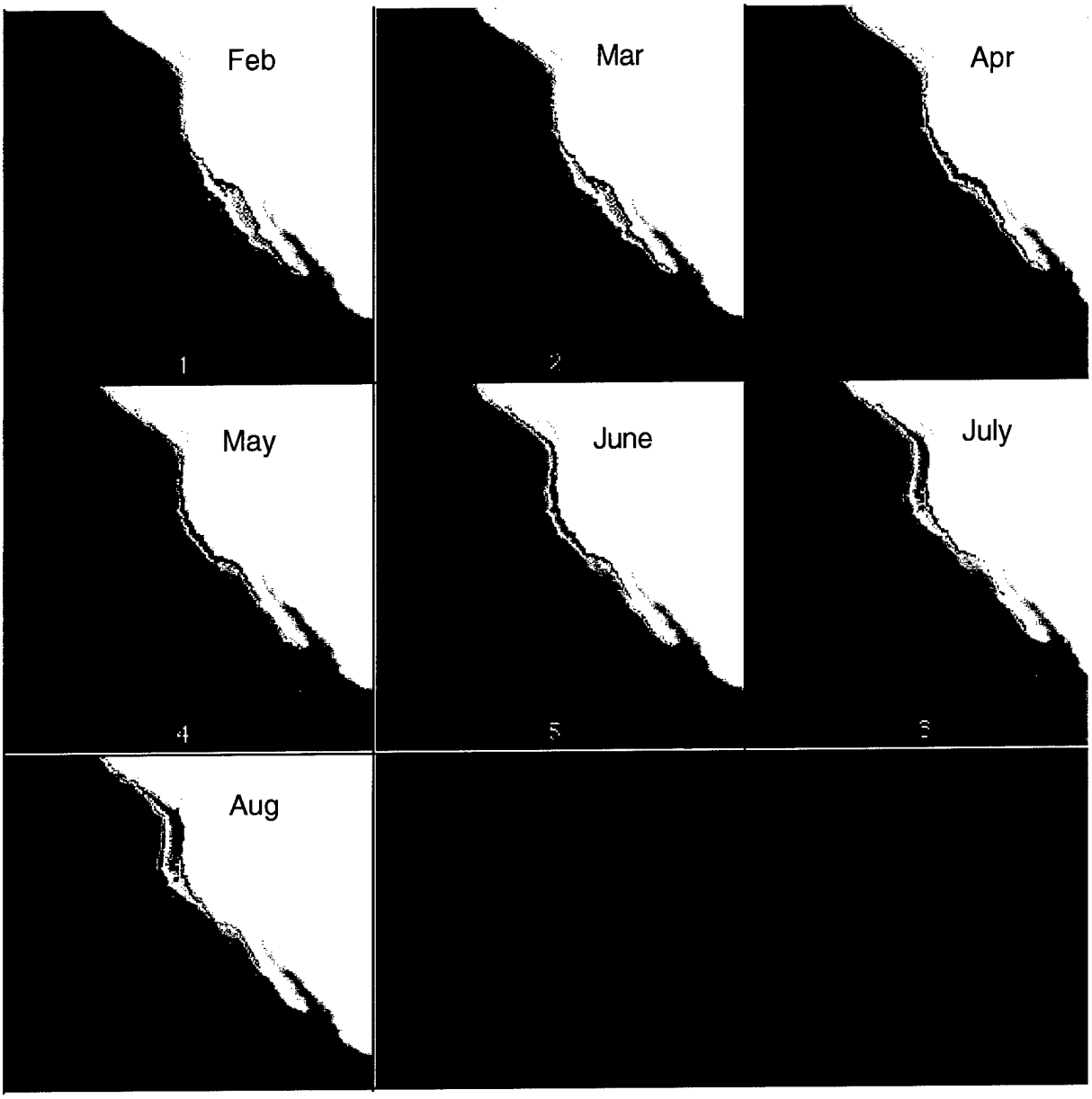

Fig. 7 — Layer scattering strength (dB) for the modified 1992 hake population, February through August, overlaid on bathymetry. The layer strength color scale ranges from red (-34 dB) to blue (-80 dB).

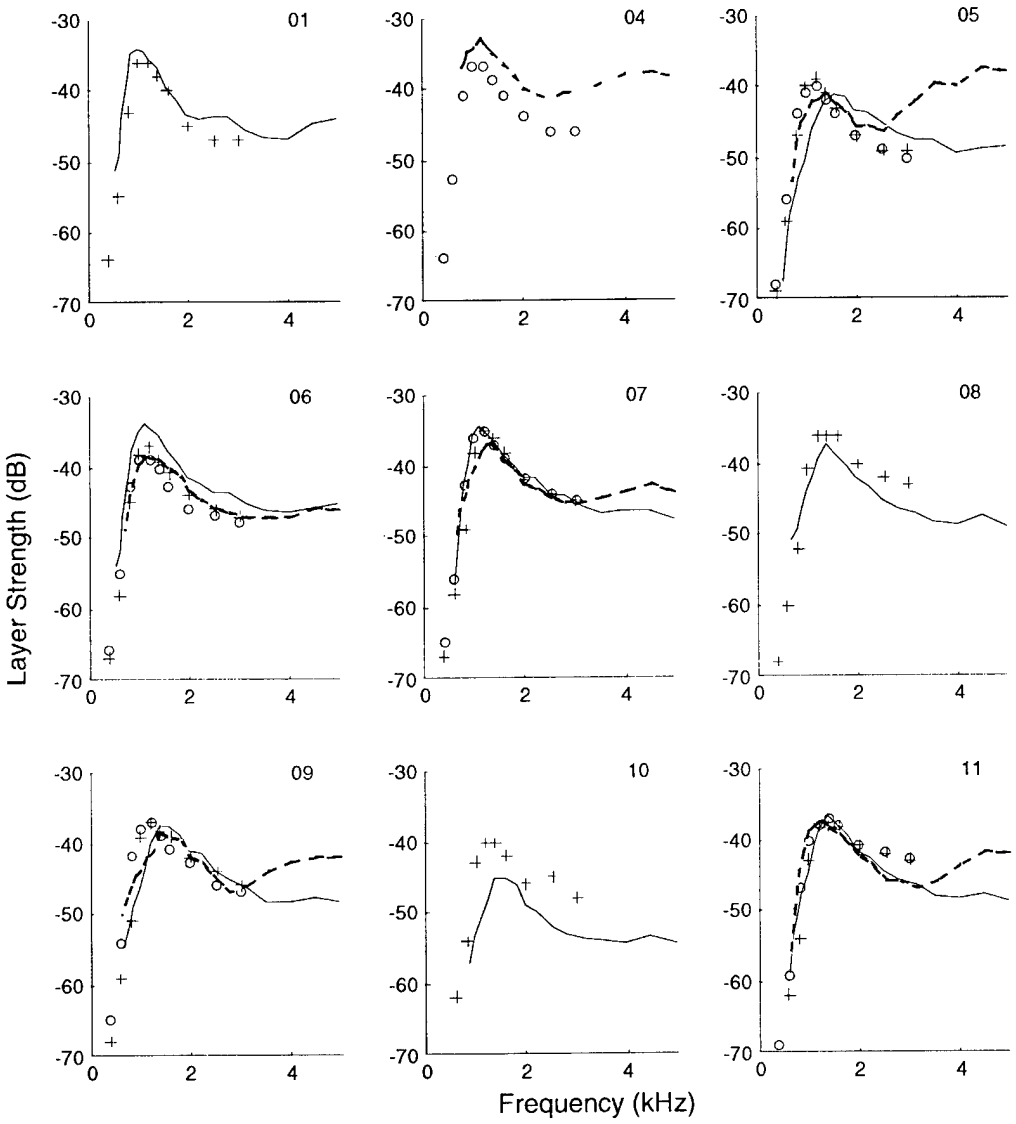

Fig. 8 — Volume scattering comparison for 1992 stations. The solid lines indicate day measurements and the dashed lines indicate night measurements. The plus symbols indicate data from the day model, and the open circles indicate data from the night model.

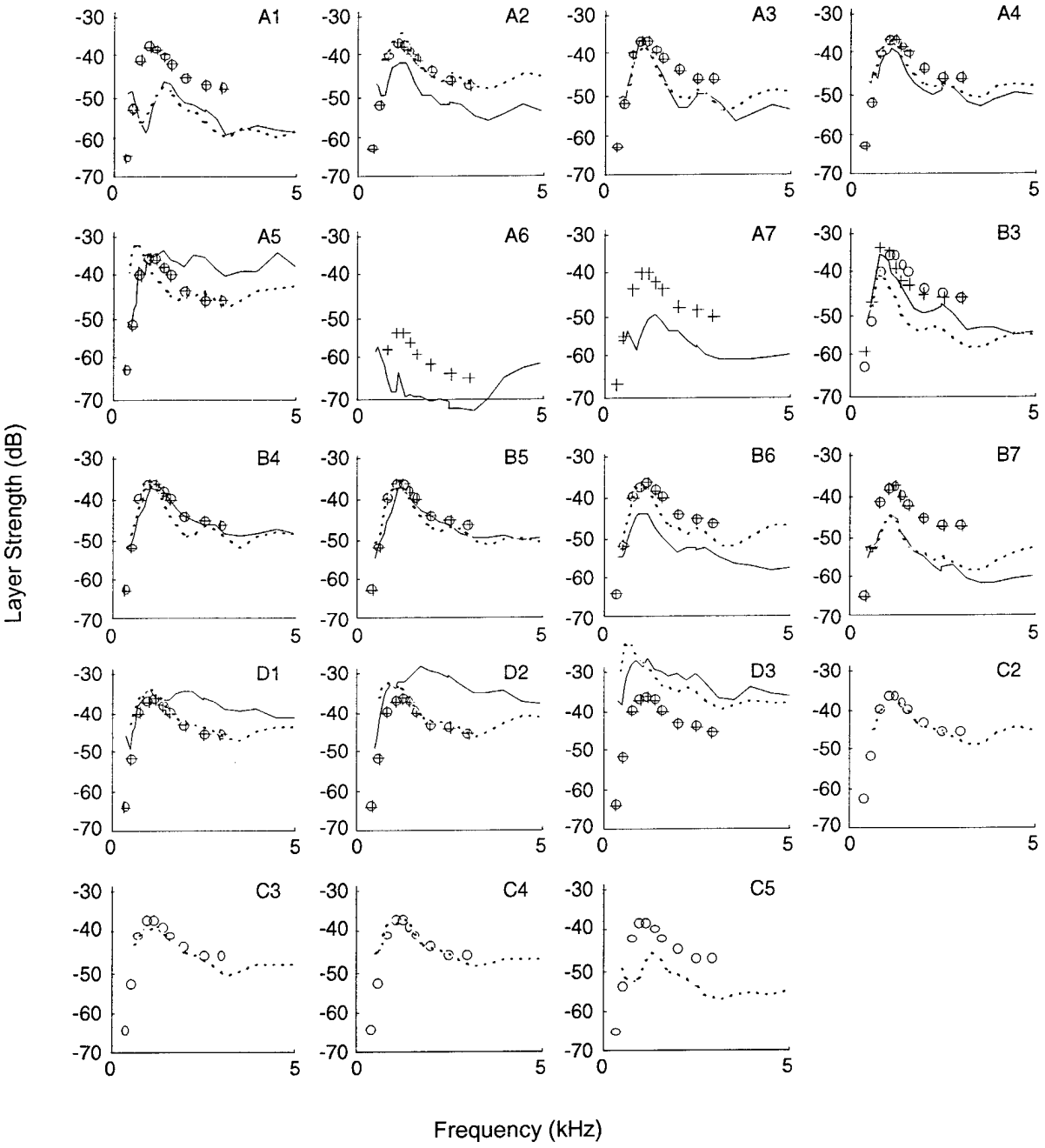

Fig. 9 — Volume scattering comparison for 1995 stations. The solid lines indicate day measurements and the dashed lines indicate night measurements. The plus symbols indicate data from the day model, and the open circles indicate data from the night model.

DISCUSSION

Volume scattering predictions using the hake migration model are comparable to within a few dB of the major features of the volume scattering data. However, for some locations this comparison can be very poor. In the most extreme cases (Stations D1 and D3), there was a 10-dB disparity between the model and the data. Some of this disparity is caused by our inability to properly fit the model to the observations because the observations contain random variations caused by the stochastic nature of the distribution of fish. Thus, predictions using this model need to be qualified with a margin of error of at least ± 3 dB. In addition, an extremely simple model was used to model the hake migration. For example, the extreme 10-dB disparity is not surprising because the modeled migration may not necessarily follow what the hake actually do.

The seasonal aspects of the hake migration are poorly known. There is no volume scatter data available from seasons other than midsummer, so the hypothesized spring, fall, and winter distributions and levels of scatter can only be judged based on the anecdotal information from the fishery. Measurements of volume scatter are needed in these other seasons to determine the accuracy of the model throughout the year.

The model fails to include several features of the behavior of Pacific hake that have recently come to light. First, it appears certain age classes of hake remain at sea in distinct schools or shoals spread over large areas (Nero et al. 1998). Such behavior will be very difficult to model because of the multitude of stochastic events that affect fish behavior. Second, during their summer feeding, hake are now known to accumulate on oceanographic upwelling sites where they feed on accumulations of Euphausiids (Mackas et al. 1997). Future modeling could encompass such behavior, but only through the inclusion of oceanographic databases or models with much more sophistication than GDEM.

Several hypotheses have been made on the mechanics of hake migration. One hypothesis suggests that they spend more time at depth in the poleward-flowing California Undercurrent to move northward, and more time in the near-surface southward-flowing California Current to move southward (C. Wilson, NMFS, Seattle, WA, pers. comm.). Such migration-based vertical positioning could be accommodated in the model presented here if at sea observations of hake prove this hypothesis.

Fluctuations in climate could be included in the model. Spawning and feeding endpoints could be increased or decreased to reflect year-to-year changes in climate. For example, if the distribution of hake moves northward during a warm event, then the model could approximate this by placing the summer feeding and winter spawning locations farther north. During the strong El Niño in summer 1998, hake were found as far north as Juneau, Alaska (59° N) (N. Williamson, NMFS, Seattle, WA, personal communication).

The basic structure of the model developed here could be adopted to describe other migrations such as those on a known route between known endpoints such as along a temperature isotherm or a depth contour, or those based on historical information. An example of a fish stock where this model could be implemented is the Norwegian Sea blue whiting. Both the winter spawning and summer feeding distributions are known, as is information on general location of the migration pathway (reviewed in Love 1993). In all cases, the quality of the modeling is dependent on the amount of information available on a particular fish stock. In some locations, this information may at best be only anecdotal.

The present model gives the mean level of volume scattering at a pixel. The next step is to include biological target information. This could be accomplished by adding school information as a subset of statistics on the schooling characteristics of hake. For example, once the density of fish at a pixel is predicted by the model, stochastic models could then be used to predict the probability of detecting false targets of a particular target strength for a given ensonified area.

The present model is useful for predicting the location, depth, and seasonal pattern of scattering on a shelf-wide basis. The model can potentially provide useful predictions of volume scatter for locations where measurements have not been made. This model represents the first step in an effort aimed at providing up-to-date information on a very dynamic and problematic subject. Further efforts should

provide mathematical refinements and additional flexibility to allow application to a variety of environments.

SUMMARY

A model has been developed to predict the vertical distribution and density of Pacific hake at monthly intervals over the extent of their range. A swimbladder scattering model is applied to predictions of hake depth and density to generate maps of volume scattering. Volume scattering predictions compare reasonably well, to within ± 3 dB of measurements made in the summers of 1992 and 1995.

Some discrepancies of up to 10 dB exist between the model and the data. Greater complexity in fish behavior and migration and interactions with oceanographic features are suggested as reasons for the discrepancies. Several suggestions are made for improvements.

Overall, the model is recommended as useful for generalized volume scattering predictions over shelf-wide geographic areas in seasons or locations where volume scattering data are sparse. Such predictions should prove beneficial in Navy planning.

ACKNOWLEDGMENTS

The author wishes to thank numerous scientists with the Alaska Fisheries Science Center, Seattle, Washington, and the Pacific Biological Station, Nanaimo, British Columbia, who answered numerous questions about the behavior and habits of Pacific hake and kindly provided results from their research. This research was supported by the Office of Naval Research.

REFERENCES

Beamish, R.J. and G.A. McFarlane, "Pacific Whiting, *Merluccius Productus*, Stocks off the West Coast of Vancouver Island, Canada," *Mar. Fish. Rev.* **47**, 75-81 (1985).

Dorn, M.W. and M.W. Saunders, "Status of the Coastal Pacific Whiting Stock in U.S. and Canada in 1977," Alaska Fisheries Science Center, miscellaneous report, 1997.

Dorn, M.W., E.P. Nunnallee, C.D. Wilson, and M.E. Wilkins, "Status of the Coastal Pacific Whiting Resource in 1993," NOAA Technical Memorandum NMFS-AFSC-47, 1994.

Ermakov, Y.K., "The Biology and Fishery of Pacific Hake, *Merluccius Productus*," Ph.D. thesis, *Pac. Sci. Inst. Mar. Fish. Oceanogr.* (TINRO), Vladivostok, USSR [English translation], 1974.

Francis, R.C., "Population and Trophic Dynamics of Pacific Hake (*Merluccius Productus*)," *Can. J. Fish. Aquat. Sci.* **40**, 1925-1943 (1983).

Francis, R.C. and A.B. Hollowed, "History and Management of the Coastal Fishery for Pacific Whiting, *Merluccius Productus*," *Mar. Fish. Rev.* **47**, 95-98 (1985).

Love, R.H., "Resonant Acoustic Scattering by Swimbladder-Bearing Fish," *J. Acoust. Soc. Am.* **64**, 571-580 (1978).

Love, R.H., "A Comparison of Volume Scattering Strength Data with Model Calculations Based on Quasisynoptically Collected Fishery Data," *J. Acoust. Soc. Am.* **94**, 2255-2268 (1993).

MacCall, A.D., *Dynamic Geography of Marine Fish Populations* (University of Washington Press, Seattle,1990).

Mackas, D.L., R. Kieser, M. Saunders, D.R. Yelland, R.M. Brown, and D.F. Moore, "Aggregation of Euphausiids and Pacific Hake (*Merluccius Productus*) along the Outer Continental Shelf off Vancouver Island," *Can. J. Fish. Aquat. Sci.* **54**, 2080-2096 (1997).

Methot, R.D. and M.W. Dorn, "Biology and Fisheries of North Pacific Hake (*M. Productus*)," in *Hake: Biology, Fisheries, and Markets*, A. Jurgen and T.J. Pitcher, eds. (Chapman and Hall, London, 1995).

Nelson, M.O. and T.A. Dark, "Results of the Coastal Pacific Whiting, *Merluccius Productus*, Surveys in 1977 and 1980," *Mar. Fish. Rev.* **47**, 82-94 (1985).

Nero, R.W., C.H. Thompson, and R.H. Love, "Low-Frequency Acoustic Measurements of Pacific Hake, *Merluccius Productus*, off the West Coast of the United States," *Fish. Bull.* **96**, 329-343 (1998).

Pitcher, T.J. and J. Alheit, "What Makes a Hake? A Review of the Critical Biological Features that Sustain Global Hake Fisheries," in *Hake: Biology, Fisheries and Markets,* A. Jurgen, and T.J. Pitcher, eds. (Chapman and Hall, London, 1995).

Saunders, M.W. and G.A. McFarlane, "Observations on the Spawning Distribution and Biology of Offshore Pacific Hake (*Merluccius Productus*)," *California Cooperative Fisheries Investigation Reports* **38**, 147-157 (1997).

Simard, Y. and D.L. Mackas, "Mesoscale Aggregations of Euphausiid Sound Scattering Layers on the Continental Shelf of Vancouver Island," *Can. J. Fish. Aquat. Sci.* **46**, 1238-1249 (1989).

Smith, B.D., G.A. McFarlane, and M.W. Saunders, "Inferring the Summer Distribution of Migratory Pacific Hake (*Merluccius Productus*) from Latitudinal Variation in Mean Lengths-at-Age and Length Frequency Distributions," *Can. J. Fish. Aquat. Sci.* **49**, 708-721 (1992).

Stauffer, G.D., "Biology and Life History of the Coastal Stock of Pacific Whiting, *Merluccius Productus*," *Mar. Fish. Rev.* **47**, 2-7 (1985).

Swartzman, G., "Analysis of the Summer Distribution of Fish Schools in the Pacific Eastern Boundary Current," *ICES J. Mar. Sci.* **54**, 105-116 (1977).

Thompson, C. H. and R. H. Love, "Determination of Fish Size Distributions and Areal Densities Using Broadband Low-Frequency Measurements," *ICES J. Mar. Sci.* **53**, 197-201 (1996).

Wilson, C.D. and M.A. Guttormsen, "Echo Integration-Trawl Survey of Pacific Whiting, *Merluccius Productus*, off the West Coasts of the United States and Canada During July-September 1995," NOAA Technical Memorandum NMFS-AFSC-74, June 1997.